Atmospheric Parameterization of Evaporation from Non-Plant-covered Surfaces

ZHUOJIA YE* AND ROGER A. PIELKE

Department of Atmospheric Science, Colorado State University, Fort Collins, Colorado

(Manuscript received 24 February 1992, in final form 22 January 1993)

ABSTRACT

A new atmospheric parameterization formulation of evaporation from a non-plant-covered surface was derived by combining the previous two types of widely used formulations, the so-called "α method" and the "β method." The study indicates that the "α method" cannot provide a reasonable estimation of evaporation from bare soil, while the "β method" does provide reasonable predictions during the daytime. However, the evaporation rate differences, estimated by the β method from that by the new parameterization, is evident at night. The deviation rises while increasing the atmospheric stability and reducing the soil wetness. The impact of atmospheric stability, soil wetness at the top or inside the soil, and soil type on evaporation rate is also discussed in detail.

1. Introduction

The earth's surface is covered by water (oceans, lakes, rivers, etc.) and different types of soil, which in turn is partly covered by vegetation with the remainder being bare. The soil has different volumetric soil water contents, as a temporary or long-term feature caused by irrigation and heterogeneously distributed precipitation, and by topographical difference. Properly estimating the dependence of evaporation from the ground surface on soil water content is important in expressing the atmosphere and surface interaction and is required in numerical weather and climate models ranging from the global scale to the microscale. Charney et al. (1977), and Shukla and Mintz (1982) indicated that the results from climate model experiments were very sensitive to the soil parameterization. Smith et al. (1986) have shown the importance of near-surface moisture content in the energy budget in a desert area. Three methods of parameterization of evaporation rate E_0 from the surface have been used as summarized in Table 1 and listed as follows:

$$E_0 = \rho_d \frac{\alpha q^{\text{sat}}_{(T_g)} - q_a}{r_a}, \tag{1}$$

$$E_0 = \rho_d \beta \frac{q^{\text{sat}}_{(T_g)} - q_a}{r_a}, \tag{2}$$

and the combined form of Eqs. (1) and (2):

$$E_0 = \rho_d \beta \frac{\alpha q^{\text{sat}}_{(T_g)} - q_a}{r_a}, \tag{3}$$

where T_g is the temperature at the ground surface, q^{sat} is the specific humidity at the saturation condition, q_a is the specific humidity of the air, and ρ_d is the air density. Variable r_a is a resistance to water vapor diffusion in air, defined as

$$r_a = \int_{Z_{0q}}^{Z_a} \frac{1}{K_q} dZ + \frac{0.0962}{k_0 u_*} \left(\frac{Z_{0q} u_*}{\nu}\right)^{0.45},$$

in which K_q is the turbulent exchange coefficient at the height Z; Z_{0q} and Z_a are aerodynamic roughness for water vapor (Verma 1989) and reference height within the surface flux layer, respectively; k_0 is the von Kármán constant; ν is the kinematic viscosity of air; and u_*, the friction velocity. The first and second terms on the right-hand side of this equation relate, respectively, to turbulent and molecular exchange processes in the turbulent layer above Z_{0q} and in the laminar layer below. A detailed derivation of this equation is provided in the Appendix.

Nappo (1975) examined the two methods expressed by Eqs. (1) and (2) with the α and β expressions as follows:

$$\alpha = h_s = \exp\left(\frac{\psi g}{R T_g}\right) \tag{4}$$

and

$$\beta = m = \frac{\theta}{\theta^{\text{sat}}}, \tag{5}$$

* Permanent affiliation: Institute of Atmospheric Physics, Chinese Academy of Sciences, Beijing, China.

Corresponding author address: Dr. Roger A. Pielke, Department of Atmospheric Science, Colorado State University, Fort Collins, CO 80523.

TABLE 1. Three methods of atmospheric parameterization of evaporation rate from soil, E_0, used in papers.

$\frac{\rho_d}{r_d}[\alpha q^{sat}_{(T_g)} - q_a]$	$\frac{\rho_d}{r_a}\beta[q^{sat}_{(T_g)} - q_a]$	$\frac{\rho_d}{r_a}\beta[\alpha q^{sat}_{(T_g)} - q_a]$
$\alpha = \exp\left[-\frac{ga}{RT_g(X_p m_g)^N}\right]$, where a, N are constants depending on soil type, (Sasamori 1970).	$\beta = 1.0 - \exp(-56.6X_p m_g)$, (Davies and Allen 1973)	$\alpha = \exp\left(\frac{g\psi}{RT_g}\right)$
$\alpha = \exp\left(\frac{\psi g}{RT_g}\right)$, (Nappo 1975)	$\beta = m_g$, [Nappo 1975 and Segal et al. (1990)]	$\beta = \left(1 + \frac{r_{soil}}{r_a}\right)^{-1}$
$\alpha = \min\left(1, \frac{1.8X_p m_g}{0.30 + X_p m_g}\right)$, (Barton 1979)*	$\beta = \min\left(1, \frac{4}{3} m_g\right)$, (Deardorff 1978)	$r_{soil} = 4140X_p(1 - m_g) - 805$ (Camillo and Gurney 1986)*
$\alpha = \min\left(1, \frac{1.8X_p m_g}{0.4 + 0.7X_p m_g}\right)$, (Yasuda and Toya 1981)*	$\beta = \left(1 + \frac{r_{soil}}{r_a}\right)^{-1}$	(Dorman and Sellers 1989)*
$\alpha = \begin{cases} 0.5\left[1 - \cos\left(\frac{\pi m_g}{m_{fc}}\right)\right], & m_g < m_{fc} \\ 1, & \text{otherwise,} \end{cases}$ (Jacquemin and Noilhan 1990)	$r_{soil} = 3.5m_g^{-2.3} + 33.5$ (Sun 1982)*	$\beta = a + \frac{1 - a}{1 + \exp[bX_p(m_t - m_g)]}$
	$r_{soil} = 3.8113 \times 10^4 \times \exp(-13.515m_g/m_{fc})$, (Passerat 1986)*	a, b, and m_t are empirical constants depending on soil type. (Avissar and Mahrer 1988)
	$r_{soil} = F/D_r$	
	$F = F_1[X_p(1 - m_g)]^{F2}$ F_1, F_2 are constants, depending on soil type, (Kondo et al. 1990)	
	$\beta = \begin{cases} 0.25\left[1 - \cos\left(\frac{\pi m_g}{m_{fc}}\right)\right]^2, & m_g < m_{fc} \\ 1, & m \geq m_{fc}, \end{cases}$ (Lee and Pielke 1992)	

* After Mahfouf and Noilhan (1991).

where ψ is the soil water potential; g is the gravity acceleration; R, the gas constant for water vapor; θ, the volumetric water content of the soil; θ^{sat}, the value of θ at the saturation condition (i.e., the volumetric fraction of soil pores, χ_p, are completely filled with water); h_s is the relative humidity in the pores; and m is soil moisture availability.

As indicated by Lee and Pielke (1992), the value of h_s computed using Philip's (1957) formulation [Eq. (4)] will be *overestimated* when the soil moisture availability drops to around the soil wilting point. Therefore the evaporation from soils under these conditions, estimated using Eq. (1) with the α value computed by Eq. (4), will also be overestimated. The disadvantage related to Eq. (2) is that the negative surface evaporation rate, which occurs over areas such as a desert area next to the ocean or a snowmelt area (Wang and Mitsuta 1991), cannot be expressed properly by Eq. (2). The negative surface evaporation rate can occur more easily using Eq. (1) than Eq. (2) (Nappo 1975). Mahfouf and Noihan (1991) indicated after comparing various formulations of evaporation from bare soil using observational data that Eqs. (1) and (2) can provide comparable results during the daytime, while significant differences are exhibited at night.

Another disadvantage concerning evaporation rate from a bare soil surface using Eqs. (1) or (2) is that the value of E_0 is independent of χ_p (which is 0.395 for sandy soil and 0.863 for peat soil!). On the other hand, when the values of m, T_g, q_a, and r_a are kept the same, E_0 from sand and from peat are equal. However, the saturated water content contained in peat soil pores is over two times as large as that in sandy soil. The values of E_0, predicted by Eqs. (1) and (2) cannot be distinguished between ocean and saturated soil if we assume T_g, q_a, and r_a keep the same values for both cases.

It is discussed in this paper that Eq. (3) has the ability to overcome this disadvantage. Furthermore, many authors (such as Barton 1979; Yasuda and Toya 1981; Camillo and Gurney 1986; Dorman and Sellers 1989; Avissar and Mahrer 1988; and Kondo et al. 1990) have indicated the dependence of E_0 on χ_p. Some of them (such as Kondo et al. 1990; Avissar and Mahrer 1988; and Ritchie 1972) also indicated that the evaporation rate from soil depends upon soil type and soil hydraulic

properties. However, the impact of χ_p on E_0 in some formulations presented by Sasamori (1970), Davies and Allen (1973), Barton (1979), and Yasuda and Toya (1981) (see Table 1) shows that E_0 increases as χ_p increases. In contrast, the dependence of E_0 on χ_p in other formulations presented by Avissar and Mahrer (1988), Dorman and Sellers (1989), and Kondo et al. (1990) is just the opposite. These issues motivate us to reexamine the parameterization of evaporation from soil.

The purpose of the current study is to provide a new evaporation formulation from a bare ground surface, which can overcome the disadvantages indicated previously and is able to explain why the β method can provide reasonable results during the daytime but exhibits significant differences at night.

2. Parameterization formulation of evaporation over bare soil

Soil consists of minerals, organic matter (which forms soil particles), water (which fills the soil pores by capillary force), and air located within the remainder of the soil pores. The vapor flux rising from the soil surface into the air directly above relates to two processes: the evaporation from the water surface (E_{0w}) contributed by the volumetric ground surface water content, θ_g, associated with a very thin upper soil layer ΔZ_0; and vapor diffusion from the remainder of the pores ($\chi_p - \theta_g$) into the overlying air, E_{0v}. The evaporation rate from θ_g is formulated as

$$E_{0w} = \rho_d \frac{q^{\text{sat}}_{(T_g)} - q_a}{r_a}, \tag{6}$$

where T_g is the soil surface temperature associated with a very thin upper layer, ΔZ_0, and computed approximately from a surface energy balance equation.

The vapor flux by a diffusion process from a pore's surface into the air is expressed as

$$E_{0v} = \rho_d \frac{q_s - q_a}{r_a}, \tag{7}$$

where q_s is the specific humidity at the soil surface. Note that the same resistance in Eqs. (6) and (7) was assumed, since the resistance is controlled by the same atmospheric characteristics with scales that are much larger than the scale of soil pores, and q_a is the value at the blending height (Wieringa 1986). Furthermore, we assumed that the mixing between E_{0w} and E_{0v} may be unimportant below the blending height.

Within the soil pores, vapor flux transported from a thin layer of depth ΔZ_1 upward by molecular diffusion is computed by

$$E_{1v} = \rho_d \frac{h_s(\theta_1) q^{\text{sat}}_{(T_{s1})} - q_s}{r_D}, \tag{8}$$

where θ_1 and T_{s1} are the volumetric soil water content and temperature averaged within a thin soil layer, ΔZ_1, next to the very thin upper soil layer; ΔZ_0 and r_D, the soil resistance to water vapor diffusion is defined as

$$r_D = \int_{(\Delta Z_1/2 + \Delta Z_0)}^{\Delta Z_0/2} \frac{1}{D_v} dZ. \tag{9}$$

The molecular diffusivity of water vapor, D_v, is expressed as (Campbell 1985)

$$D_v = D_{v0} \left(\frac{T}{T_{00}}\right)^2 \left(\frac{p_{00}}{p}\right), \tag{10}$$

where $T_{00} = 273.15$ K and $P_{00} = 1013$ mb are the temperature and air pressure at standard conditions near sea level, and $D_{v0} = 21.7$ mm^2 s^{-1} is the value of D_v at these standard conditions (Campbell 1985).

Assume that the total water vapor flux across any cross section within the soil pores is in (quasi-steady) equilibrium. Therefore, we have

$$S_a(g) E_{0v} = S_a(1) E_{1v}, \tag{11a}$$

where $S_a(g)$ and $S_a(1)$ are the area fraction of air averaged at ΔZ_0 and ΔZ_1, respectively. It is evident that $S_a(g) = \chi_p(g) - \theta_g$, and $S_a(1) = \chi_p(1) = \chi_p(1) - \theta_{(1)}$. Therefore, Eq. (11a) becomes

$$[\chi_p(g) - \theta_g] E_{0v} = [\chi_p(1) - \theta_{(1)}] E_{1v}. \tag{11b}$$

By neglecting the water vapor flux contributed from the fraction area occupied by solid soil particles [$1 - \chi_p(g)$], the total water vapor flux over a soil surface can be approximated as

$$E_0 = \theta_g E_{0w} + [\chi_p(g) - \theta_g] E_{0v}. \tag{12a}$$

Inserting Eqs. (7) and (8) into Eq. (11b) and reorganizing it result into an expression of q_s:

$$q_s = \frac{q_a + \dfrac{\chi_p(1) - \theta_{(1)}}{\chi_p(g) - \theta_g} \left[\dfrac{r_a}{r_D} h_s(\theta_1) q^{\text{sat}}_{(T_{s1})}\right]}{\left[1 + \dfrac{\chi_p(1) - \theta_{(1)}}{\chi_p(g) - \theta_g} \dfrac{r_a}{r_D}\right]}. \tag{12b}$$

Substituting Eq. (12b) into Eq. (7) and inserting the resultant expression along with Eq. (6) into Eq. (12a), yields

$$E_0 = \frac{\rho_d}{r_a} \beta [\alpha q^{\text{sat}}_{(T_g)} - q_a], \tag{13}$$

where

$$\beta = \chi_p(g) - \frac{[\chi_p(g) - \theta_g]}{1 + \dfrac{\chi_p(1) - \theta_{(1)}}{\chi_p(g) - \theta_g} \dfrac{r_a}{r_D}}, \tag{14}$$

and

$$\alpha = \frac{1}{\beta}\left[\theta_g + \frac{\chi_p(1) - \theta_{(1)}}{1 + \dfrac{\chi_p(1) - \theta_{(1)}}{\chi_p(g) - \theta_g}\dfrac{r_a}{r_D}} \frac{r_a}{r_D} h_{s(\theta_1)} \frac{q^{\text{sat}}_{(T_{s1})}}{q^{\text{sat}}_{(T_g)}}\right]. \quad (15)$$

3. Results and discussion

The previous formulations of evaporation from the soil surface, expressed by Eqs. (1) and (2), are called the "α method" and "β method," respectively. The present parameterization formulation, given by Eq. (13), is a combination form which we refer to as the "α and β method." A similar version with different expressions of α and β has been presented in Table 1.

a. The impact of ratio r_a/r_D and soil moisture availability on β

Equation (14) divided by χ_p yields

$$\beta_* = \frac{\beta}{\chi_p(g)} = 1 - \frac{1 - m_g}{1 + \dfrac{\chi_p(1)}{\chi_p(g)}\dfrac{1 - m_{(1)}}{1 - m_g}\dfrac{r_a}{r_D}}, \quad (16)$$

where m is the soil moisture availability, defined by Eq. (5).

A representative value of r_D is 400 s m^{-1}. The value of r_a is dependent on Z_{0q}, ambient wind speed, and atmospheric thermal stability, ranging from 10^2 s m^{-1} under very stable stratified atmospheric conditions with a very smooth ground surface, to about 10^0 s m^{-1} in a very rough surface under unstable conditions. Therefore the ratio r_a/r_D changes its values from 10^0 in very stable conditions to 10^{-2} under very unstable situations. For a given soil type and soil wetness condition, Eq. (16) describes that (a) when the ratio of r_a/r_D increases (i.e., when the atmospheric thermal stability tends to be more stable or less unstable) β_* increases; (b) for given soil types and a ratio of r_a/r_D, the value of β_* decreases as the drying process proceeds in initially wet soil, because of the reduction of the value m_g and the increment of $[1 - m(1)]/(1 - mg)$; (c) generally $\beta_* < 1$, but $\beta_* \to 1$ when $m_g \to 1$; and (d) generally, $\beta_* > m_g$, but $\beta_* \to m_g$ when $r_a/r_D \to 0$.

Figure 1 presents the impact of r_a/r_D on β_* for three different values of m_g; m_g = 0.05 (profile A), 0.25 (profile B), and 0.5 (profile C), respectively, under the assumption that soil type and soil moisture availability were uniformly distributed (this assumption is used in all figures presented below). It illustrates that the impact of r_a/r_D on β_* intensifies as soil moisture availability decreases. When soil moisture is small (m = 0.05, for example), the value of β_* expands its value by an order of magnitude when r_a/r_D increases from 0.01 to 1.0 (see profile A). The relatively abrupt alteration of β_* with r_a/r_D occurs with relatively smaller values of r_a/r_D.

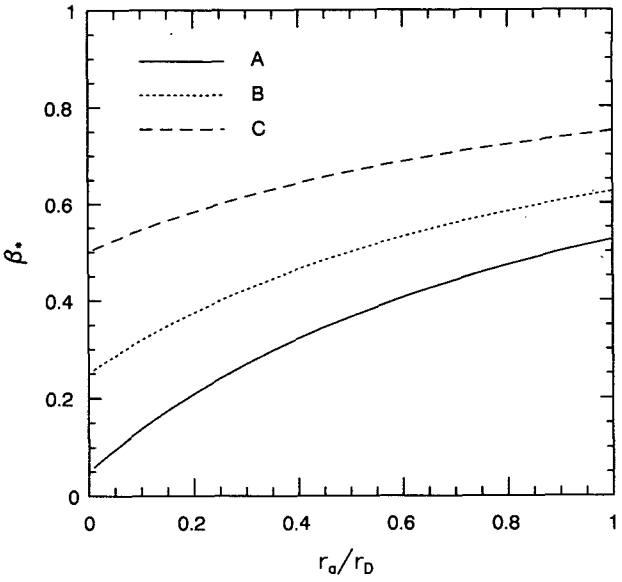

FIG. 1. The dependence of β_* on r_a/r_D for m_g = 0.05 (profile A), 0.25 (B), and 0.5 (C), respectively, with the assumption that the soil type and soil moisture availability were uniformly distributed.

The dependence of β_* on m_g and $m_{(1)}$ can be explored by differentiating Eq. (16) with respect to m_g and $m_{(1)}$, respectively,

$$\frac{d\beta_*}{dm_g} = 1 - \left[\frac{\dfrac{r_a}{r_D}\dfrac{1 - m_{(1)}}{1 - m_g}\dfrac{\chi_p(1)}{\chi_p(g)}}{1 + \dfrac{r_a}{r_D}\dfrac{1 - m_{(1)}}{1 - m_g}\dfrac{\chi_p(1)}{\chi_p(g)}}\right]^2, \quad (17)$$

and

$$\frac{d\beta_*}{dm_{(1)}} = -\frac{r_a}{r_D}\frac{\chi_p(1)}{\chi_p(g)}\left[1 + \frac{\chi_p(1)}{\chi_p(g)}\frac{r_a}{r_D}\frac{1 - m_{(1)}}{1 - m_g}\right]^{-2}. \quad (18)$$

Equation (17) indicates that (a) the slope $d\beta_*/dm_g$ is always positive, since the second term on the right-hand side of Eq. (17) is less than one; (b) the slope increases as the value of r_a/r_D decreases; and (c) when $r_a/r_D \ll 1$, $d\beta_*/dm_g \to 1$.

Equation (18) describes that (a) since the value on the right-hand side of Eq. (18) is negative for any values of r_a/r_D and $1 - m_{(1)}/(1 - m_g)$, the value of β_* always reduces as the soil moisture availability increases inside the soil layer; (b) the slope, $-d\beta_*/dm_{(1)}$, is generally less than one; and (c) the slope, $-d\beta_*/dm_{(1)}$ will linearly increase with r_a/r_D under the condition $r_a/r_D \ll 1$.

Figure 2, computed from Eq. (16) with r_a/r_D = 1.0 (profile A), 0.1 (profile B), and 0.01 (profile C), respectively, and the other conditions as used in Fig. 1,

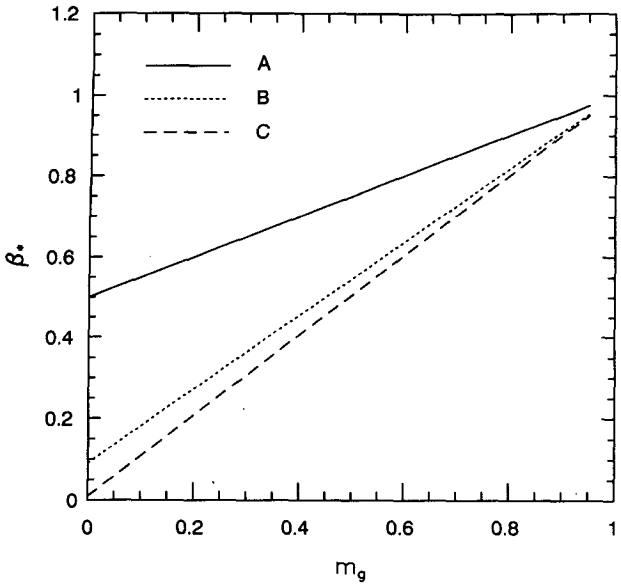

FIG. 2. The dependence of β_* on soil moisture availability for r_a/r_D = 0.01 (profile C), 0.1 (B), and 1.0 (A), respectively, with the same assumption as in Fig. 1.

illustrates that the value of β_* increases linearly with the value of m_g. When the value of r_a/r_D is small (profile C), β_* is approximately equal to m_g. The deviation of β_* from $m_g(\beta_* > m_g)$ increases as the atmospheric stability increases for a fixed value of m_g, and decreases as the soil moisture availability increases for a fixed value of r_a/r_D.

The above discussion implies that the value of β_* is dependent on both the atmospheric stability near the surface and the soil moisture availability.

b. The dependence of α on r_a/r_D and soil moisture availability

Combining Eqs. (15) and (16), to eliminate β results in

$$\alpha = \frac{1}{\beta_*}\left\{ m_g + \frac{[1 - m_{(1)}]\dfrac{\chi_p(1)}{\chi_p(g)}}{1 + \dfrac{\chi_p(1)}{\chi_p(g)}\dfrac{1 - m_{(1)}}{1 - m_g}\dfrac{r_a}{r_D}} \times \frac{r_a}{r_D}\frac{q^{\text{sat}}_{(T_{s1})}}{q^{\text{sat}}_{(T_g)}} h_{s[m_{(1)}]} \right\}. \quad (19)$$

The value of h_s as dependent on m is computed using the formulation given by Jacquemin and Noilhan (1990):

$$h_s(m) = \begin{cases} 0.5\left[1 - \cos\left(\pi \dfrac{m}{m_{fc}}\right)\right], & \text{if} \quad m \leqslant m_{fc} \\ 1, & \text{otherwise,} \end{cases} \quad (20)$$

where the subscript f_c stands for field capacity of soil. The values of m_{fc} for different soil types can be found from Lee and Pielke (1992) and Cosby et al. (1984).

Figure 3, computed based on Eq. (19), presents the dependence of α on r_a/r_D for three cases of soil moisture availability: m_g = 0.05 (profile A), 0.25 (profile B), and 0.5 (profile C) under the conditions that the soil type, soil moisture availability, and soil temperature are distributed uniformly, with m_{fc} = 0.366 for loamy sand soil (Lee and Pielke 1992).

For m_g = 0.05, the value of α decreases nonlinearly from about 0.85 to about 0.13 when r_a/r_D increases from 0.01 to 1.0. When the soil moisture availability increases, the dependence of the value of α on r_a/r_D is weakened. When the soil moisture availability is greater than m_{fc}, the value of α is equal to one, which is independent of r_a/r_D. The value of α = 1 when $r_a/r_D \to 0$ for any value of m_g.

Figure 4 illustrates the impact of m_g on α for three cases of r_a/r_D = 1.0 (profile A), 0.1 (profile B), and 0.01 (profile C) with the same conditions as indicated in Fig. 3. The profile D presents the dependence of h_s on m_g computed based on Eq. (20). It shows that (a) for any values of r_a/r_D, increasing the soil moisture availability results in the increase of α when $m < m_{fc}$; when $m \geqslant m_{fc}$, we have α = 1; (b) the gradient of α with respect to m_g is sharpened as the value of r_a/r_D decreases (or as the atmospheric instability increases); and (c) comparing profile D with profiles A, B, C indicates that $\alpha > h_s$, when $m_g < m_{fc}$. The deviation of α from h_s increases as the value of r_a/r_D is decreased, which means that when the atmospheric stability tends to be more stable, the α profile will approach the h_s profile.

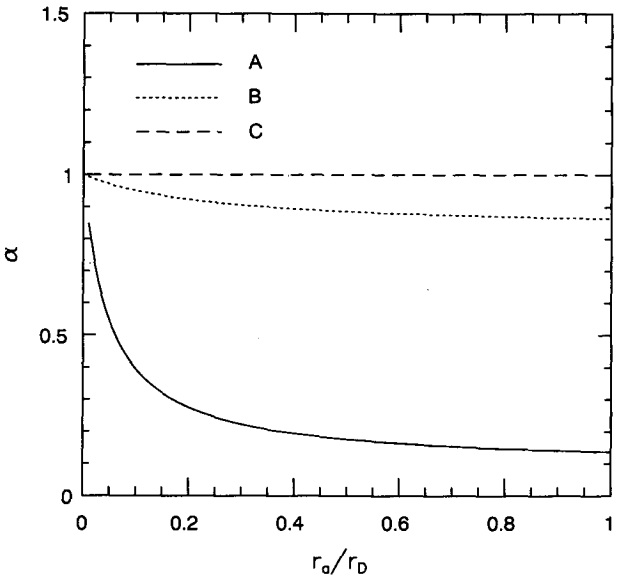

FIG. 3. The same as in Fig. 1 except for α instead of β_*.

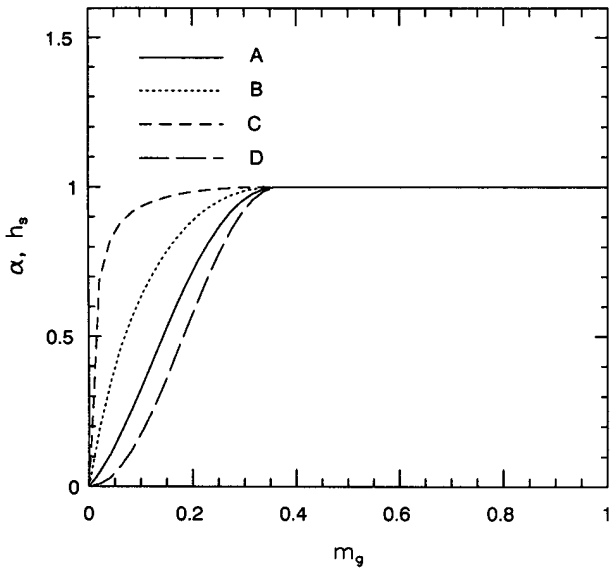

FIG. 4. The same as in profiles A, B, and C of Fig. 2 except for α instead of β_* where profile D was computed based on Eq. (20) for comparison of α with h_s.

It suggests that when the soil moisture availability is greater than the soil field capacity or $r_a/r_D \to 0$, $\alpha = 1$, and Eq. (13) becomes the β method.

c. The impact of r_a/r_D, and m on E_0

Equation (13) can be expressed as

$$E_0 = \frac{\rho_d}{r_a}\beta(\alpha - hh_c)q^{\text{sat}}_{(T_g)}, \tag{21}$$

where h is the atmospheric relative humidity, defined as

$$h = \frac{q_a}{q_a^{\text{sat}}} \quad \text{and} \tag{22}$$

$$h_c = \frac{q_a^{\text{sat}}}{q^{\text{sat}}_{(T_g)}}. \tag{23}$$

The value of h_c is dependent on the air temperature deviation from the surface temperature (i.e., on the atmospheric thermal stability).

Equation (21) indicates that (a) for fixed values of h, h_c, α, β, and r_a, higher temperature corresponds to a higher value of q^{sat}, which results in a higher value of E_0; (b) there will be no water vapor flux when

$$hh_c = \alpha; \tag{24}$$

and (c) during the daytime, the atmospheric thermal stability is in an unstable condition, $h_c < 1$. The value of h_c decreases as atmospheric instability increases. Generally, $\alpha > hh_c$ holds, so $E_0 > 0$. The value of E_0 increases as the atmospheric relative humidity h decreases, and/or the atmospheric instability increases (i.e., decreasing the value of h_c), and/or the soil moisture availability increases, which increases both values of α and β, as discussed in sections 3a and 3b. Note that the value of α decreases as the value of r_a/r_D increases (increasing the stability) and/or the soil moisture availability decreases. Therefore, under a suitable condition (dry soil with overlying humid air), even in the daytime, a negative vapor flux (i.e., condensation) will be able to occur; and (d) at night, a surface radiative inversion is formed, which results in increasing both values, r_a and h_c ($h_c > 1$), and the value of h is enhanced because the temperature drops. As compared to the daytime situation, $E_0 < 0$ at night is able to occur more easily. Turbulent intensity characterized by r_a^{-1} at night is usually one order of magnitude smaller than during the day. Therefore, the value of E_0 at night is commonly smaller as compared to that during the day.

Figure 5 presents an example of the impact of r_a/r_D on E_* in three cases, $m = 0.05$ (profile A), 0.25 (profile B), and 0.5 (profile C), under conditions $r_D = 400$ s m^{-1}, $T_g = 26$°C, and $T_a = 22$°C, $h = 60\%$, during the day (Fig. 5a) and $T_g = 22$°C, $T_a = 26$°C, $h = 71\%$ at night, for a loamy sand soil uniformly distributed, where $E_* = E_0/\rho_d\chi_p$. Figure 5a illustrates the dependence of E_* (m s^{-1}) on r_a/r_D during the day. It illustrates that the values of E_* for the three cases decrease by one order of magnitude when the value of r_a/r_D increases from 0.01 to 0.1. A sharper decrease occurs when $r_a/r_D \geq 0.02$. A negative value of E_* during the day is computed for a very dry soil with $m_g = 0.05$ and $r_a/r_D \geq 0.076$. However, the value of E_* is very small, since the turbulence is weak. Therefore, $E_* > 0$ is common during the daytime.

At night (Fig. 5b), both $E_* > 0$ and $E_* < 0$ are computed with the given conditions indicated above. The dependence of the absolute values of E_* on r_a/r_D at night exhibits the same rule as that during the day. However, the positive and negative water vapor fluxes at night are much smaller than those during the day. When the soil is dry ($m_g = 0.05$) with a high air relative humidity ($h = 71\%$) and inversion intensity is 4°C, condensation occurs (profile A). The amount of condensation water increases as the turbulent intensity increases (i.e., decreasing the value of r_a/r_D). When the soil moisture availability $m_g = 0.5$ is above the soil field capacity, under the same given conditions, the values of E_* are positive. When $m_g = 0.25$, the value of E_* decreases from positive to negative when the value of r_a/r_D increases from 0.12 to 1.0. The transition point is at about $r_a/r_D = 0.4$ for the given condition, which will decrease as the soil moisture availability decreases or both values of the air relative humidity and the inversion intensity increase.

Figure 6a depicts the impact of soil moisture availability on E_* for three values of $r_a = 4$ s m^{-1} (profile D), $r_a = 40$ s m^{-1} (profile C) during the day, $r_a = 40$

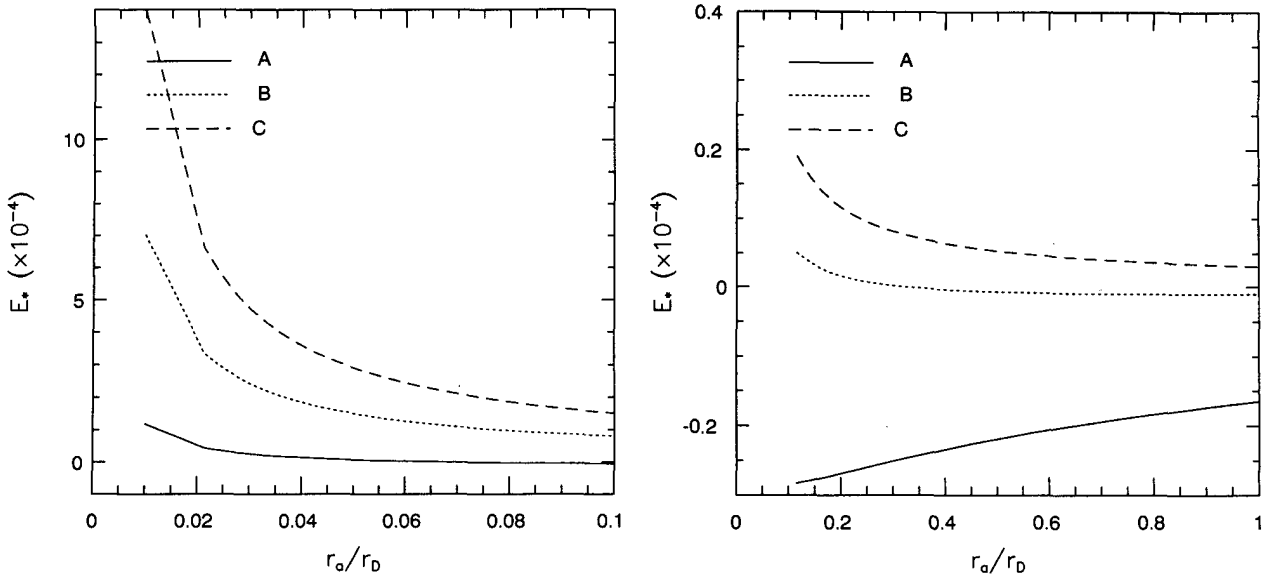

FIG. 5. The impact of r_a/r_D on E_* (m s^{-1}), with r_D = 400 s m^{-1}, p = 1000 mb, for m_g = 0.05 (profile A), 0.25 (B) and 0.5 (C), respectively, under the conditions, loamy sand soil with moisture availability uniformly distributed and T_g = 26°C, T_a = 22°C, h = 60% for (a); and T_g = 22°C, T_a = 26°C, h = 71% for (b).

s m^{-1} (profile B), and r_a = 400 s m^{-1} (profile A) at night under the same conditions as indicated in Fig. 5. Figure 6b is a higher resolution portion of Fig. 6a. It illustrates that during the day, except under very dry soil conditions ($m_g \leq 0.05$), the value of E_* is positive, and it increases rapidly with increasing value of m_g. The value of E_* increases from 1.17 × 10^{-4} m s^{-1} at m_g = 0.05 to 2.6 × 10^{-3} m s^{-1} at m_g = 0.95 in the case of r_a = 4 s m^{-1}. Negative vapor flux can occur during the day only in a very dry soil condition as illustrated in Fig. 6b. The value of m_g, at which the vapor flux is changed from negative to positive, increases as the atmospheric turbulent intensity decreases (the transition value of $m_g \approx 0.007$ when $r_a \rightarrow 4$ s m^{-1} and m_g = 0.06, while r_a = 40 s m^{-1} is computed as shown by profiles C and D in Fig. 6b). The transition

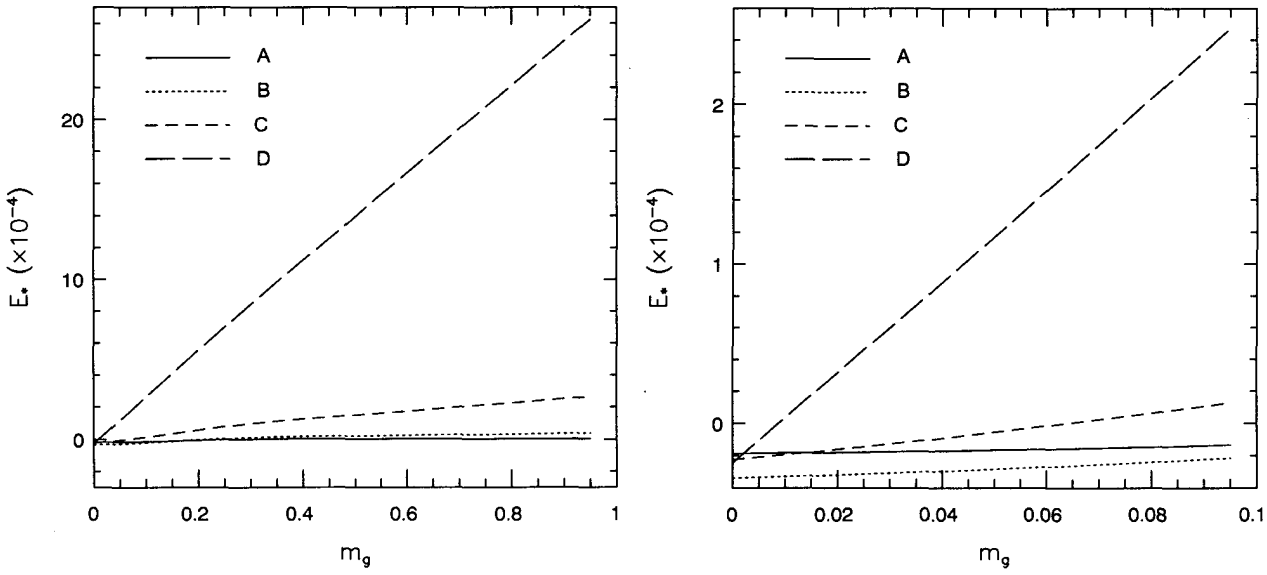

FIG. 6. (a) The dependence of E_* (m s^{-1}) on soil moisture availability for r_a/r_D = 0.01 (profile D), 0.1 (profile C) during the day, r_a/r_D = 0.1 (profile B), and 1.0 (profile A) at night, respectively, with the other conditions the same as used in Fig. 5. (b) A magnification of the lower-left portion of (a).

point of m_g also increases as the humidity of the overlying air increases. The gradient of E_* with respect to m_g is much sharper as compared to the change of E_* with r_a/r_D. The reason is that when the value of m_g increases, both values of α and β_* increase rapidly, as shown by Figs. 2 and 4. However, when the value of r_a/r_D increases, the value of β_* increases, but the value of α decreases, as shown by Figs. 1 and 3. At night, the value of E_* changes its sign at $m_g \approx 0.225$ for $r_a = 40$ s m^{-1} and at $m_g \approx 0.275$ for $r_a = 400$ s m^{-1} for the given conditions, which suggests that for this situation, weak turbulence favors the occurrence of condensation. The amount of condensation water decreases, however, as the soil wetness increases and/or the turbulent intensity decreases. Figure 6 also illustrates that at night the values of E_* are much smaller as compared to the values during the day. The dependence of E_* on m_g is linear, but on r_a/r_D is nonlinear as illustrated by Figs. (5) and (6).

d. Discussion

Combining Eqs. (13), (16), and (23) yields

$$E_0 = \rho_d \chi_p(g) \beta_* \frac{[\alpha q_{(T_g)} - q_a]}{r_a}, \tag{25a}$$

$$E_0 = \rho_d \chi_p(g) \beta_* \frac{(\alpha - hh_c) q^{\text{sat}}_{(T_g)}}{r_a}. \tag{25b}$$

Equation (25) indicates that for fixed values of β_*, α, T_g, q_a, and r_a (i.e., for fixed values of T_g, ΔT, q_a, and r_a), the water vapor flux from (or to) the ground surface is linearly proportional to the soil porosity volumetric fraction under the condition that the soil type is unchanged within a shallow soil layer, because both α and β_* in this condition are independent of χ_p. When $\chi_p(g) \neq \chi_p(1)$, E_0 nonlinearly depends on $\chi_p(g)$. This result is different from the previous evaporation formula given by Nappo (1975), Deardorff (1978), Jacquemin and Noilhan (1990), and others (see Table 1 for details). In these formulas of evaporation, the evaporation rate is the same for peat soil ($\chi_p = 0.863$) and sand soil ($\chi_p = 0.395$), which is unreasonable. The dependence of E_0 on χ_p given by the present parameterization qualitatively agrees with that given by Sasamori (1970), Davies and Allen (1973), Barton (1979), and Yasuda and Toya (1981) (see Table 1 for details).

Since the new formula contains the dependence of E_0 on $\chi_p(g)$, Eq. (25) can be extended to estimate the evaporation rate from free open water bodies (such as rivers, lakes, and oceans). These free open water bodies can be imagined as a special soil with $\chi_p(g) = m = 1$. Under this condition, β_* and α, computed from Eqs. (16) and (19), are equal to 1. Therefore, Eq. (25) used to estimate the evaporation rate from a free open water body simplifies to

$$E_0 = E_w = \frac{\rho_d}{r_a} [q^{\text{sat}}_{(T_g)} - q_a]. \tag{26}$$

The above discussion suggests that for given values of T_g, q_a, and r_a, the evaporation rate from an open water body is larger than that from any type of soil even under saturated soil water condition. Penman (1948) provided experimental data measured from two cylinders filled with water and a sandy loam, respectively, which supports this opinion. He indicated that the evaporation rate from wet bare soil with an adequate supply of water is obtained as a fraction of that from open water. However, the surface roughness length over soil is commonly much larger than that over free open water bodies, and T_g for soil is higher in daytime than that for free open water under the same overlying environmental conditions. That is why the evaporation rate measured over soil can be larger than that from an adjacent water body during the day.

It is necessary to clarify that Eq. (25) describes the water vapor flux at the surface, not the evaporation rate from the surface. These are equal for a soil surface with $m_g = 1.0$ or over an open water body. In the case that $m_g < 1$, however, the value of E_0 consists of two portions; one is evaporated from θ_g which consumes latent heat and will take part in the heat balance equation at the surface. The remainder of E_0 is contributed by vapor diffusion through soil pores as the vapor is evaporated at different depths of the soil and will, therefore, take part in the heat balance equation at different depths of the soil.

From the discussion in sections 3a and 3b, except for $m_g = 1$ the values of β_* are always less than one. Therefore the α method can never be reached. However, on some occasions, α is equal to or approaches one and the β method is a good approximation to Eq. (25). These occasions include (a) when the soil moisture availability is about equal to or greater than the soil field capacity (see Fig. 4 for details). In this soil wetness condition, the value of β_* is about equal to the value of m_g, when $r_a/r_D \leq 0.1$, as shown by profiles B and C in Fig. 2. When the value of r_a/r_D increases, the deviation of β_* from m_g also increases, as illustrated by profile A in Fig. 2; $\beta_*/m_g = 1.9$ was computed under the conditions $r_a/r_D = 1.0$, $m_g = m_{fc}$, as shown by Fig. 2; and (b) from Eqs. (16) and (19), when $r_a/r_D \ll 1$, $\beta_* \approx m_g$ and $\alpha \approx 1$ can be derived. These features can also be seen from Figs. 1 and 3. Figures 1 and 3 illustrate that when $r_a/r_D \leq 0.035$, the values of α and β_* are as follows: $\alpha = 1.0$, $\beta_* = 0.505$–0.517 for $m_g = 0.5$; $\alpha = 0.97$–0.993, $\beta_* = 0.257$–0.276 for $m_g = 0.25$; and $\alpha = 0.622$–0.849, $\beta_* = 0.059$–0.083 for $m_g = 0.05$. This discussion indicates that for the conditions of $r_a/r_D \leq 0.035$, $m_g \geq 0.25$ (about 70% of m_{fc})

the values of α and β_* can be expressed as $\alpha = 1$ and $\beta_* \approx m_g$ [i.e., Eq. (5) holds]. That is to say that under these conditions, Eq. (25) is simplified to a β method. For a representative value of $r_D = 400$ s m^{-1}, $r_a/r_D \leq 0.035$ implies $u_* \geq 0.2$ m s^{-1} in neutral atmospheric condition when we set $r_a^{-1} \approx ku_*$. A value of $u_* \geq 0.2$ m s^{-1} is common in daytime unstable boundary conditions.

In order to further estimate the accuracy of the computed water vapor flux using the β method, the following equation can be derived from Eq. (25):

$$F_\beta = \frac{E_0 - E_{0\beta}}{E_0} = \frac{\alpha - 1}{\alpha - hh_c} \tag{27}$$

where E_0 is expressed by Eq. (25), $E_{0\beta}$ is expressed by Eq. (25) with $\alpha = 1$. Then, the accuracy of the β method is determined by the value of F_β as follows; for $F_\beta < 0$, the β method provides an overestimate, for $F_\beta > 0$, the β method is an underestimate, while for $F_\beta = 0$, the β method is accurate.

From the discussion above, the values of α computed based on Eq. (19) were from 0.9 to 0.98 with $m_g = 0.2$ when r_a/r_D changed its values from 0.1 to 0.01 during the day (i.e., $\alpha \to 1$ when $r_a/r_D \to 0$), and $\alpha = 1$ for any value of r_a/r_D when $m_g \geq m_{fc}$. However, $\alpha < 1$ when the value of r_a/r_d increases under the condition of $m_g < m_{fc}$. It suggests that during the daytime for situations of low synoptic wind and cloudless skies, the β method is a good approximation of Eq. (25). It will fail when the atmospheric turbulent intensity decreases and the soil is in a very dry condition during the day. For this condition, when $hh_c < \alpha < 1$, $F_\beta < 0$, and the β method overestimates the evaporation from the soil, alternatively $F_\beta > 0$ when $\alpha < hh_c < 1$, so that the β method underestimates the evaporation from the soil, but it occurs only rarely during the day because of the need for small values of h and h_c.

At night, the β method is accurate only under the condition of $m_g \geq m_{fc}$ and $\alpha \neq hh_c$. For the remainder of the conditions, however, $\alpha < 1$ which is already shown by Fig. 3. The deviation of α from 1 for a given $m_g < m_{fc}$ increases as r_a/r_D increases, suggesting $|F_\beta|$ is larger at night as compared with that during the day for the same conditions. On the other hand, the values of h_c range from 1 to 1.7 as ΔT changes from 0 to 10 K, computed based on Eq. (23). The decreased temperature at night makes h increase after sunset. Therefore situations of $\alpha < hh_c < 1$ and $hh_c < \alpha < 1$ are equally likely. Further, $F_\beta > 0$, which occurs in favorable conditions of relatively dry soil or large values of r_a/r_D (both result in a smaller value of α), or strength inversion (which yields a larger value of h_c), and increasing relative humidity.

The results can be used to qualitatively explain Mahfouf and Noilhan's (1991) conclusions. They indicated after discussing the β method based on in situ data collected over a silty clay loam bare soil, with soil surface moisture availability decreasing from field capacity to dry conditions that, during the daytime, it provided comparable results as contrasted to observed data while significant differences were exhibited at night. They also indicated, based on comparing the accumulated evaporation values that, computed by the β method (e.g., tests 2 and 3 in their paper) and deduced from both observed water budget and aerodynamic measurements, the β method (tests 2 and 3) gives quite similar results and clearly overestimates the integrated evaporation value as a consequence of the assumption $h = \alpha = 1$. Since the evaporation rate during the daytime is one order of magnitude larger than that at night as mentioned above, we can anticipate that the accumulated evaporation rate estimated using the β method will be overestimated based on Eq. (27).

The above procedure can also be applied to estimate the accuracy of the α method, where the α method is the formulation of Eq. (25) with $\beta_* = 1$. Then we have

$$F_\alpha = \frac{E_0 - E_{0\alpha}}{E_0} = 1 - \frac{1}{\beta_*}, \tag{28}$$

with $E_{0\alpha}$ the evaporation rate computed with the α method.

When $F_\alpha > 0$, the α method underestimates the evaporation from a bare soil, while with $F_\alpha < 0$, the α method overestimates the evaporation. Figures 1 and 2 illustrate that $\beta_* < 1.0$ at any value of r_a/r_D and m_g, except $m_g = 1.0$ (where, $\beta_* = 1$). Therefore, Eq. (28) suggests that the α method always overestimates evaporation. The overestimation decreases with increasing values of r_a/r_D and m_g as shown in Figs. 1 and 2.

4. Conclusions

In the present study, a new parameterization formulation of water vapor flux at the interface between air and an underlying non-plant-covered ground surface was derived. The new formulation is a combination of previous α and β formulations. The present study also investigated the sensitivity of the impact of r_a/r_D and m_g on α, β, and E_0. The major conclusions we obtained from this study follow.

- Based on the results computed from Eq. (16), over unsaturated soil the value of β_* was always less than one during the daytime and at night. Therefore, the α method cannot provide a reasonable prediction of evaporation from bare soil; the α method always overestimates the evaporation rate from unsaturated soil.
- The β method can provide as good a prediction in estimating the daytime evaporation rate as the one computed by Eq. (25). However, the evaporation rate estimated by the β method will deviate significantly from that predicted by Eq. (25) at nighttime. Overestimation or underestimation can occur at night de-

pending on whether α is greater or smaller than hh_c. The difference increases when the soil is drier.

- The new parameterization formula of evaporation from a bare soil is explicitly dependent on soil type as indicated by soil porosity unlike the α and β methods. This formula can also be used to estimate the evaporation over open water bodies (such as lakes and oceans) by setting $\chi_p = 1.0$.
- The values of α and β_* are sensitive to the atmospheric stability and soil moisture availability. When the atmospheric stability and/or the soil moisture availability increases, the value of β_* rises. The value of α is reduced as the atmospheric stability increases or the soil moisture availability is reduced. The impacts of r_a/r_D on α and β_* intensify as the soil moisture availability decreases. The influence of soil moisture availability on α and β_* becomes more important as the availability decreases. The influence of soil moisture availability on α and β_* becomes more important as the atmospheric instability increases.
- The sign of water vapor flux near the surface depends on the value of $\alpha - hh_c$. During the day, negative vapor flux can occur only under very dry soil conditions ($m_g \leqslant 0.06$ when $r_a/r_D = 0.1$ and $m_g \leqslant 0.007$ when $r_a/r_D = 0.01$ were computed with $h = 60\%$). At night, however, negative vapor flux occurs more easily as compared to daytime ($m_g < 0.225$ for $r_a/r_D = 0.1$ and $m_g < 0.275$ for $r_a/r_D = 1$ were computed with $h = 71\%$). The absolute value of E_0 during the day is an order of magnitude larger than at night since the value of r_a at night is one order of magnitude larger than that during the day. The absolute value of E_0 is proportional to m_g and decreases nonlinearly with r_a/r_D. The impact of m_g on E_0 is more sensitive as compared to the impact of r_a/r_D, since α and β_* increase as the value of m_g increases; however, as r_a/r_D increases, β_* increases but α decreases.

Acknowledgments. This study was supported by NSF Grant ATM-8915265. We would like to thank T. Smith and D. McDonald for the preparation of the manuscript, and X. Zeng for the preparation of figures.

APPENDIX A

Derivation of r_a

The expression for the deviation of q_s at the interface between soil and air from $q(Z_{0q})$ as a function of u_*, q_*, Z_{0q}, and ν, based on Zilitinkevich (1970) is

$$q_s - q_{(Z_{0q})} = -0.0962 \frac{q_*}{k_0} \left(\frac{u_* Z_{0q}}{\nu} \right)^{0.45},$$

$$= -0.0962 \frac{u_* q_*}{k_0 u_*} \left(\frac{u_* Z_{0q}}{\nu} \right)^{0.45}, \quad \text{(A1)}$$

where q_* is the turbulent scaling parameter for water vapor.

The water vapor fluxes within the laminar layer ($0 < Z < Z_{0q}$), $\rho_d[q_s - q(Z_{0q})]/r'$ and in the surface flux layer, $-\rho_d u_* q_* = \rho_d[q(Z_{0q}) - q_a]/r'_a$ are equal under equilibrium conditions, where

$$r'_a = \int_{Z_{0q}}^{Z_a} \frac{1}{k_q} dZ; \quad \text{(A2)}$$

so that for r' and E_0 we have

$$r' = \frac{0.0962}{k_0 u_*} \left(\frac{Z_{0q} u_*}{\nu} \right)^{0.45}, \quad \text{(A3)}$$

$$E_0 = \rho_d \frac{q_s - q_a}{r_a}, \quad \text{(A4)}$$

$$\text{where} \quad r_a = r'_a + r'. \quad \text{(A5)}$$

For typical values of $u_* \sim 10^0 \sim 10^1$ cm s^{-1}, Z_{0q} for soils $0.1 \sim 1$ cm, and $\nu = 0.15$ cm^2 s^{-1}, for r' we have $r' \approx 1/k_0 u_*$. In a neutral or stable condition, $r'_a \sim (c/k_0 u_*) \ln(Z_a/Z_{0q})$, where $c = K_m/K_q$, is the ratio of turbulent exchange coefficients for momentum and water vapor.

REFERENCES

Avissar, R., and Y. Mahrer, 1988: Mapping forest-sensitive areas with a three-dimensional local-scale numerical model. Part I: Physical and numerical aspects. *J. Appl. Meteor.*, **27**, 400–413.

Barton, I. J., 1979: A parameterization of the evaporation from non-saturated surfaces. *J. Appl. Meteor.*, **18**, 43–47.

Camillo, P. J., and R. J. Gurney, 1986: A resistance parameter for bare soil evaporation models. *Soil Sci.*, **141**, 95–105.

Campbell, G. S., 1985: *Soil Physics with Basic.* Elsevier Science Publishers, 150 pp.

Charney, J. G., W. J. Quirk, S. H. Chow, and J. Komfield, 1977: A comparative study of the effects of albedo change on drought in semi-arid regions. *J. Atmos. Sci.*, **34**, 1366–1385.

Cosby, B. J., G. M. Hornberger, R. B. Clapp, and T. R. Ginn, 1984: A statistical exploration of the relationships of soil moisture characteristics to physical properties of soil. *Water Resour. Res.*, **20**, 682–690.

Davies, J. A., and C. D. Allen, 1973: Equilibrium, potential and actual evaporation from cropped surfaces in southern Ontario. *J. Appl. Meteor.*, **12**, 649–657.

Deardorff, J. W., 1978: Efficient prediction of ground temperature and moisture with inclusion of a layer of vegetation. *J. Geophys. Res.*, **83**, 1889–1903.

Dorman, J. L., and P. J. Sellers, 1989: A global climatology for albedo, roughness length, and stomatal resistance for atmospheric general circulation models as represented by the simple biosphere model (SiB). *J. Appl. Meteor.*, **28**, 833–855.

Jacquemin, B., and J. Noilhan, 1990: Sensitivity study and validation of land surface parameterization using the HAPEX-MOBILHY data set. *Bound.-Layer Meteor.*, **52**, 93–134.

Kondo, J., N. Saigusa, and T. Sato, 1990: A parameterization of evaporation from bare soil surface. *J. Appl. Meteor.*, **29**, 385–389.

Lee, T. J., and R. A. Pielke, 1992: Estimating the soil surface specific humidity. *J. Appl. Meteor.*, **31**, 480–484.

Mahfouf, J. F., and J. Noilhan, 1991: Comparative study of various formulations of evaporation from bare soil using in situ data. *J. Appl. Meteor.*, **30**, 1354–1365.

Nappo, C. J., 1975: Parameterization of surface moisture and evaporation rate in a planetary boundary layer model. *J. Appl. Meteor.*, **14,** 289–296.

Passerat de Silans, A., 1986: Transfert de masse et de chaleur dans un sol stratifé soumis à une excitation atmosphérique naturelle. Comparaison: Modèles-expérience. Thesis, Institut National Polytechnique de Grenoble.

Penman, H. L., 1948: Natural evaporation from open water, bare soil and grass. *Proc. Roy. Soc. London,* **A193,** 120–145.

Philip, J. R., 1957: Evaporation, and moisture and heat fields in the soil. *J. Meteor.*, **14,** 354–366.

Ritchie, J. T., 1972: Model for predicting evaporation from a row crop with incomplete cover. *Water Resour. Res.*, **8,** 1204–1213.

Sasamori, T., 1970: A numerical study of atmospheric and soil boundary layer. *J. Atmos. Sci.*, **27,** 1122–1137.

Segal, M., X. Jia, Z. Ye, and R. A. Pielke, 1990: On the effect of daytime surface evaporation on pollution dispersion. *Atmos. Environ.*, **24A,** 1801–1811.

Shukla, J., and Y. Mintz, 1982: Influence of land surface evapotranspiration on the earth's climate. *Science,* **15,** 1498–1501.

Smith, E. A., E. R. Reiter, and Y. Gao, 1986: Transition of surface energy budget in the Gobi Desert between spring and summer seasons. *J. Appl. Meteor.*, **25,** 1725–1740.

Sun, S. F., 1982: Moisture and heat transport in a soil layer forced by atmospheric conditions. M.S. thesis, University of Connecticut.

Verma, S. B., 1989: Aerodynamic resistances to transfers of heat, mass and momentum. *Proc. Int. Workshop, XIX General Assembly of the Int. Union of Geodesy and Geophysics,* Vancouver, B.C., Canada, IAMS Publication No. 177, 13–20.

Wang, J., and Y. Mitsuta, 1991: Turbulence structure and transfer characteristics in the surface of the HEIFE Gobi area. *J. Meteor. Soc. Japan,* **69,** 587–593.

Wieringa, J., 1986: Roughness-dependent geographical interpolation of surface wind speed averages. *Quart. J. Roy. Meteor. Soc.,* **112,** 867–889.

Yasuda, N., and T. Toya, 1981: Evaporation from non-saturated surface and surface moisture availability. *Pap. Meteor. Geophys.,* **32,** 89–98.

Zilitinkevich, S. S., 1970: *The Dynamics of the Atmospheric Boundary Layer.* Gidrometeoizdat, 239 pp.